Received: 26 June 2020 | Revised: 8 August 2020 | Accepted: 13 August 2020

DOI: 10.1002/aoc.6028

FULL PAPER

Applied Organometallic Chemistry WILEY

An ultrasound assisted cyclocondensation reaction for the efficient synthesis of [1]benzopyranopyrido[*d*]pyrimidines using porous graphene/MoO_3

Shahrzad Abdolmohammadi[1] | **Maryam Afsharpour**[2]

[1]Department of Chemistry, East Tehran Branch, Islamic Azad University, Tehran, Iran

[2]Department of Inorganic Chemistry, Chemistry & Chemical Engineering Research Center of Iran, Tehran, Iran

Correspondence
Shahrzad Abdolmohammadi, Department of Chemistry, East Tehran Branch, Islamic Azad University, P.O. Box 18735-138, Tehran, Iran.
Email: s.abdolmohamadi@iauet.ac.ir; s.abdolmohamadi@yahoo.com

Funding information
Research Council of East Tehran Branch, Islamic Azad University

In this paper, we report a feasible protocol for the preparation of [1]benzopyranopyrido[*d*]pyrimidines via expeditious sonochemical route. The reaction efficiency was evaluated by influence of several parameters including sonication power, sonication time, different solvents, and using porous graphene/MoO_3 nanocomposite as catalyst, for the first time. The effect of the ultrasonication comparing with the conventional heating on the synthesis of the titled compounds shows that the ultrasonic irradiation is required to rich the cyclized products. The structural properties of porous graphene/MoO_3 nanocomposite were determined by Fourier transform infrared spectroscopy (FT-IR), powder X-ray diffractometry (XRD), scanning electron microscope (SEM), Raman spectroscopy, and also by TGA analysis. Confirmation of the structures of compounds **4a–4h** were also established with IR, ^{1}H NMR, and ^{13}C NMR spectroscopic data and also by elemental analyses.

KEYWORDS

[1]benzopyranopyrido[*d*]pyridines, aqueous media, porous graphene/MoO_3 nanocomposite, room temperature, ultrasonic irradiation

1 | INTRODUCTION

Introduction of ultrasonication as a versatile synthetic tool has created a new opportunity to develop new procedures in organic syntheses that cannot be achieved by conventional methods.[1–4] The ultrasound approach by providing the activation energy in microenvironment has quickly gained acceptance for accelerating assembly of complex molecules in an efficient, green, atom-economical, and time saving manner.[5–7] The avoid or reduce the use of hazardous organic solvents, which is often an intrinsic part of chemical or another industrial manufacturing process, can mainly prevented environmental pollution.[8] According to this, performing the reactions under ultrasound conditions in combination with using water as an ideal green medium instead of other popular reaction solvents is considered efficient, safe, and economically feasible treatment for convenient practice of green chemistry.[9–13]

Furthermore, metal oxide nanoparticles (NPs) can be also selected as long-term stable and efficient heterogeneous catalysts for greener synthetic approaches to important organic compounds.[14] Recently, researches have witnessed considerable attempts to develop the applications of nanostructure materials,[15] due to their broad range of applications in photocatalysts,[16,17] superhydrophobicity material,[18] organic conductors, electromagnetic interference shielding, and so on.[19] New nanocomposites have been successfully prepared based on graphitic materials thanks to their important various categories of carbon nanostructures such as fullerenes, graphene, carbon nanotubes, and nanofibers.[20] Among different graphitic supported materials, graphene-based has been emerged as powerful catalysts, because they

have high surface area, high chemical stability, high thermal conductivity, and low resistivity.[21]

The multicomponent reactions (MCRs),[22] which highlighting important contributions by combination a minimum of three reactants (or a reactant with three reaction centers) in a single step to form a product that incorporates frameworks containing substantial elements of all the reactants are well-recognized tools in macrocyclization strategies, peptide cyclization, and diversity-oriented derivatization of complex fused heterocyclic.[23]

Moreover, compounds incorporate [1]benzopyran (chromene) motives are widespread among natural and unnatural bio-active compounds.[24] Compounds caring the [1]benzopyran motif have been successfully utilized as cosmetics, pigments,[25] and potential biodegradable agrochemicals.[26] These compounds have a wide spectrum of biologically activities such as antimicrobial,[27] antiviral,[28,29] mutagenicitical,[30] antitumoral,[31] antiproliferative,[32] sex pheromonal,[33] antioxidants,[34] central nervous system activities,[35] and enzyme inhibitors.[36] Moreover, the core structure of fused [1]benzopyran is widespread in a large number of well-known medicinally relevant natural compounds. For example, uvafzlelin, as a naturally occurring 4*H*-[1]benzopyran isolated from the stems of *Uvaria ufielii*, has been identified as antimicrobial against Gram-positive and acid-fast bacteria,[37] conrauinone A has been isolated from the bark of the tree *Millettia conraui* and shown potential ability in the treatment of intestinal parasites,[38] and erysenegalensein C extracted from the bark of *Erythrina senegalensis* can be used as a drug for the treatment of stomach pain, female infertility, and gonorrhea[39] (Figure 1).

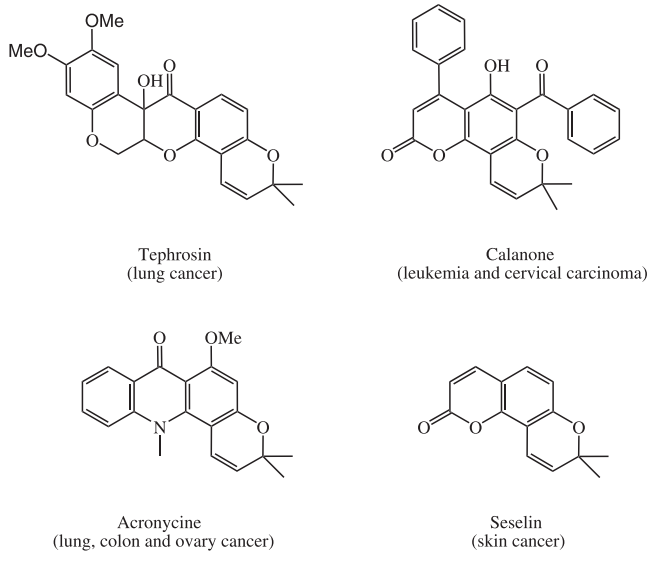

FIGURE 1 Natural biologically active compounds containing core structure of fused [1]benzopyran

We have previously developed some facile and non-polluting routes in forming heterocycles using metal oxide nanoparticles.[40] In the present work, we set out to prove the efficiency of eco-compatible ultrasonication as a practical approach for the synthesis of 7-aryl-9,-11-dimethyl-6*H*-[1]benzopyrano[3′,4′:5,6]pyrido[2,3-*d*] pyrimidine-6,8,10(9*H*,11*H*)-trione derivatives **4a**–**4h** via a three-component reaction of 4-hydroxycoumarin (**1**), aromatic aldehydes (**2**), and 6-amino-1,3-dimethyluracil (**3**) in the presence of porous graphene/MoO_3 nanocomposite as a reusable heterogeneous catalyst in aqueous media. The notable feature of this novel and promising procedure is the fact that in the absence of ultrasonic wave, the final cyclized product was not obtained even under reflux conditions (Scheme 1).

2 | EXPERIMENTAL

2.1 | Materials and methods

All of the chemical materials used in this work were purchased from Merck and Fluka and used without further purification. Melting points were determined on an Electrothermal 9100 apparatus. The FT-IR spectra were obtained from a Bruker, Vector spectrometer. ^{1}H NMR and ^{13}C NMR spectra were recorded on a Bruker DRX-500 AVANCE at 500 and 125 MHz, respectively, using TMS as internal standard and DMSO(d_6) as solvent. Elemental analyses were carried out on Foss-Heraeus CHN-O-rapid analyzer instruments. XRD patterns were obtained from Bruker Axs using CuKα radiation with $\lambda = 1.54060$ Å in the range $2\theta = 10$–80°. The SEM images were taken using scanning electron microscope TESCAN, VEGA3 equipped with the X-ray energy dispersive spectroscope (EDX). Raman spectra were derived from Bruker, Senterra micro-Raman with a laser wavelength of 785 nm. Ultrasonication was performed using on a multiwave ultrasonic generator (Sonicator 3200; Bandelin, MS-73), equipped with a converter/transducer and titanium oscillator (horn), 12.5 mm in diameter, with an operation frequency of 20 KHz with a maximum power output of 200 W.

2.2 | General procedure for the synthesis of bio-graphene

Each gelatin of 2.5 g and Arabic gum were dissolved separately in 40 ml water and stirred at 50°C until clear gel was obtained. Then, the resultant gels were mixed well under stirring. The mixture was heated to remove water and dried at 80°C for 12 h. Then, the dried powder was

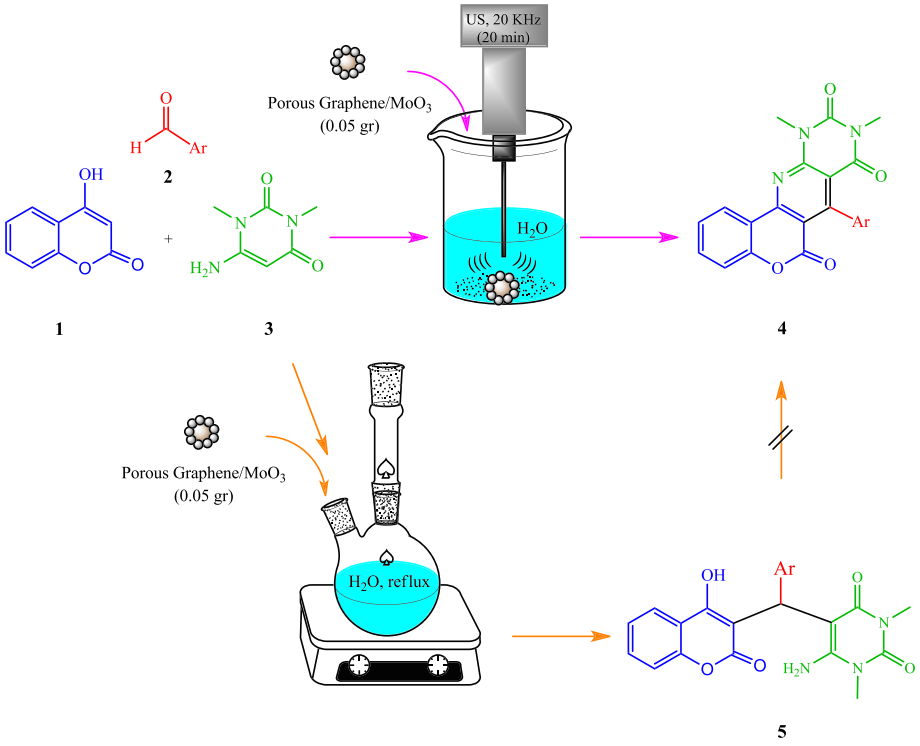

SCHEME 1 Ultrasound-assisted, porous graphene/MoO_3 nanocomposite catalyzed preparation of 7-aryl-9,11-dimethyl-6*H*-[1]benzopyrano[3′,4′:5,6]pyrido[2,3-*d*]pyrimidine-6,8,10(9*H*,11*H*)-triones in water

put in a furnace, heated to 750°C with the rate of 5°/min for 1 h at N_2 atmosphere. The product is a black powder that has a graphene structure synthesized from natural precursors.

2.3 | General procedure for the synthesis of graphene/MoO_3 nanocomposite

To immobilization of molybdenum oxide on the surface of the synthesized bio-graphene, an active aqueous solution of molybdenum was used. For this purpose, oxodiperoxo molybdenum complex was first synthesized by mixing MoO_3 (5 mmol, 0.72 g) with 5 ml of H_2O_2 (30%). The mixture was heated at 40°C for 24 h under stirring until a clear yellow solution was obtained. Then 100 mg of the synthesized bio-graphene were added to the molybdenum solution and refluxed at 100°C for 48 h under stirring. After 48 h, the solution was cooled to room temperature, centrifuged, washed with distilled water, and dried in an air oven.

2.4 | General procedure for the preparation of compounds 4a–4h

A mixture of 4-hydroxycoumarin (**1**, 1 mmol), aromatic aldehyde **2** (1 mmol), 6-amino-1,3-dimethyluracil (**3**, 1 mmol), and porous graphene/MoO_3 (0.05 gr) in H_2O (3 ml) was sonicated at room temperature for 20 min at power of 70 W. The reaction progress was monitored by TLC using 2:1 ethyl acetate/n-hexane as an eluent. After completion of the reaction, the reaction was allowed to stand for 10 min at room temperature, and then the solid obtained was filtered. The residue was then dissolved in hot ethanol (3 ml), and the catalyst was removed for reusing by centrifuging and washing with ethanol and then oven drying for several hours. The pure product was obtained by cooling the ethanol solution to room temperature, diluted with 1 ml H_2O and allowed to crystallize.

2.5 | Spectroscopic data

2.5.1 | 9,11-Dimethyl-7-phenyl-6*H*-[1]benzopyrano[3′,4′:5,6]pyrido[2,3-*d*]pyrimidine-6,8,10(9*H*,11*H*)trione (4a)

White solid, yield: 0.364 g (95%), mp >300°C. IR (KBr) (ν_{max}/cm^{-1}): 2845, 2732, 1706, 1658, 1618, 1571, 1510, 1450, 1356, 767. ^{1}H-NMR: δ = 3.26 (s, 3H, NCH_3), 3.49 (s, 3H, NCH_3), 7.47 (d, 3H, J = 7.2 Hz, H—Ar), 7.58 (d, 2H, J = 7.2 Hz, H—Ar), 7.68 (t, 1H, J = 7.2 Hz, H—Ar), 7.75 (d, 1H, J = 8.2 Hz, H—Ar), 7.97 (t, 1H, J = 7.6 Hz, H—Ar), 8.16 (d, 1H, J = 7.6 Hz, H—Ar) ppm. ^{13}C-NMR: δ = 27.1, 29.0, 105.7, 112.5, 113.9, 117.8, 121.4, 124.6, 126.6, 127.2, 129.0, 131.3, 134.6, 135.9, 140.8, 142.9, 150.9, 157.0, 169.0,

173.1 ppm. *Anal.* Calcd for $C_{22}H_{15}N_3O_4$ (385.38): C, 68.57; H, 3.92; N, 10.90. Found: C, 68.69; H, 3.82; N, 10.81.

2.5.2 | 7-(4-Bromophenyl)-9,11-dimethyl-[1]benzopyrano[3′,4′:5,6]pyrido[2,3-*d*]pyrimidine-6,8,10(9*H*,11*H*)trione (4b)

White solid, yield: 0.455 g (98%), mp >300°C. IR (KBr) (ν_{max}/cm^{-1}): 2937, 2760, 1700, 1666, 1618, 1572, 1508, 1449, 1351, 762. ^{1}H-NMR: δ = 3.25 (s, 3H, NCH_3), 3.49 (s, 3H, NCH_3), 7.34 (d, 2H, J = 8.2 Hz, H—Ar), 7.59 (d, 1H, J = 7.8 Hz, H—Ar), 7.62 (d, 2H, J = 8.2 Hz, H—Ar), 7.65 (d, 1H, J = 8.7 Hz, H—Ar), 7.88 (t, 1H, J = 7.8 Hz, H—Ar), 8.05 (d, 1H, J = 7.8 Hz, H—Ar) ppm. ^{13}C-NMR: δ = 27.7, 29.1, 105.3, 112.4, 113.1, 117.8, 122.9, 124.6, 125.0, 127.1, 128.3, 129.2, 131.7, 138.9, 140.2, 142.9, 150.7, 157.5, 170.4, 172.9 ppm. Anal. Calcd for $C_{22}H_{14}BrN_3O_4$ (464.27): C, 56.92; H, 3.04; N, 9.05. Found: C, 57.05; H, 3.21; N, 9.15.

2.5.3 | 7-(4-Chlorophenyl)-9,11-dimethyl-6*H*-[1]benzopyrano[3′,4′:5,6]pyrido[2,3-*d*]pyrimidine-6,8,10(9*H*,11*H*)trione (4c)

White solid, yield: 0.407 g (97%), mp >300°C. IR (KBr) (ν_{max}/cm^{-1}): 2952, 2871, 1689, 1668, 1619, 1570, 1511, 1443, 1355, 752. ^{1}H-NMR: δ = 3.27 (s, 3H, NCH_3), 3.50 (s, 3H, NCH_3), 7.45 (d, 2H, J = 8.1 Hz, H—Ar), 7.54 (d, 2H, J = 8.1 Hz, H—Ar), 7.63 (t, 1H, J = 7.5 Hz, H—Ar), 7.70 (d, 1H, J = 8.3 Hz, H—Ar), 7.92 (t, 1H, J = 7.6 Hz, H—Ar), 8.11 (d, 1H, J = 7.6 Hz, H—Ar) ppm. ^{13}C-NMR: δ = 27.1, 29.1, 105.4, 112.6, 114.0, 117.8, 124.6, 125.2, 127.4, 129.3, 131.2, 133.4, 134.1, 138.4, 140.8, 142.7, 150.9, 156.9, 168.8, 172.5 ppm. Anal. Calcd for $C_{22}H_{14}ClN_3O_4$ (419.82): C, 62.94; H, 3.36; N, 10.01. Found: C, 63.05; H, 3.46; N 10.13.

2.5.4 | 7-(4-Cyanophenyl)-9,11-dimethyl-6*H*-[1]benzopyrano[3′,4′:5,6]pyrido[2,3-*d*]pyrimidine-6,8,10(9*H*,11*H*)trione (4d)

Pale yellow solid, yield: 0.402 g (98%), mp >300°C. IR (KBr) (ν_{max}/cm^{-1}): 2965, 2883, 2223, 1705, 1667, 1619, 1572, 1505, 1450, 1345, 759. ^{1}H-NMR: δ = 3.26 (s, 3H, NCH_3), 3.50 (s, 3H, NCH_3), 7.73 (d, 2H, J = 8.2 Hz, H—Ar), 7.76 (d, 2H, J = 8.2 Hz, H—Ar), 7.81 (d, 1H, J = 8.3 Hz, H—Ar), 8.05 (m, 2H, H—Ar), 8.21 (d, 1H, J = 7.9 Hz, H—Ar) ppm. ^{13}C-NMR: δ = 27.2, 29.1, 105.2, 110.4, 112.6, 114.5, 117.8, 119.8, 124.0, 125.0, 128.2, 129.4, 134.5, 135.3, 139.1, 140.7, 142.6, 150.9, 156.2, 169.2, 173.0 ppm. *Anal.* Calcd for $C_{23}H_{14}N_4O_4$ (410.39): C, 67.31; H, 3.44; N, 13.65. Found: C, 67.17; H, 3.52; N, 13.49.

2.5.5 | 9,11-Dimethyl-7-(3-hydroxyphenyl)-6*H*-[1]benzopyrano[3′,4′:5,6]pyrido[2,3-*d*]pyrimidine-6,8,10(9*H*,11*H*)trione (4e)

Pale yellow solid, yield: 0.389 g (97%), mp >300°C. IR (KBr) (ν_{max}/cm^{-1}): 3436, 2923, 2758, 1678, 1651, 1620, 1570, 1510, 1445, 1353, 756. ^{1}H-NMR: δ = 3.25 (s, 3H, NCH_3), 3.51 (s, 3H, NCH_3), 7.52 (m, 2H, H—Ar), 7.65 (br s, 2H, H-Ar), 7.73 (t, 1H, J = 7.5 Hz, H—Ar), 7.79 (d, 1H, J = 8.2 Hz, H—Ar), 8.01 (t, 1H, J = 7.8 Hz, H—Ar), 8.21 (d, 1H, J = 7.8 Hz, HAr), 9.44 (s, 1 H, OH) ppm. ^{13}C-NMR: δ = 27.0, 29.1, 105.5, 112.7, 113.6, 114.1, 114.5, 117.8, 124.4, 124.7, 127.3, 130.0, 133.3, 135.9, 138.4, 140.7, 143.0, 151.0, 155.9, 166.6, 169.2, 173.1 ppm. Anal. Calcd for $C_{22}H_{15}N_3O_5$ (401.38): C, 65.83; H, 3.77; N, 10.47. Found: C, 65.68; H, 3.59; N, 10.30.

2.5.6 | 9,11-Dimethyl-7-(4-methoxyphenyl)-6*H*-[1]benzopyrano[3′,4′:5,6]pyrido[2,3-*d*]pyrimidine-6,8,10(9*H*,11*H*)trione (4f)

Yellow solid, yield: 0.407 g (98%), mp >300°C. IR (KBr) (ν_{max}/cm^{-1}): 2923, 2874, 1703, 1675, 1619, 1571, 1507, 1440, 1356, 768. ^{1}H-NMR: δ = 3.26 (s, 3H, NCH_3), 3.49 (s, 3H, NCH_3), 3.68 (s, 3H, OCH_3), 7.01 (d, 2H, J = 8.0 Hz, H—Ar), 7.27 (d, 2H, J = 8.02 Hz, H—Ar), 7.59 (t, 1H, J = 7.5 Hz, H—Ar), 7.66 (d, 1H, J = 8.2 Hz, H—Ar), 7.87 (t, 1H, J = 7.8 Hz, H—Ar), 8.06 (d, 1H, J = 7.8 Hz, H—Ar) ppm. ^{13}C-NMR: δ = 27.2, 29.1, 55.7, 105.8, 112.4, 114.0, 117.8, 123.1, 124.6, 125.2, 128.3, 129.5, 133.7, 135.3, 141.0, 142.8, 150.9, 155.9, 158.2, 167.7, 172.9 ppm. Anal. Calcd for $C_{23}H_{17}N_3O_5$ (415.40): C, 66.50; H, 4.12; N, 10.12. Found: C, 66.39; H, 3.98; N, 10.22.

2.5.7 | 9,11-Dimethyl-7-(4-methylphenyl)-6*H*-[1]benzopyrano[3′,4′:5,6]pyrido[2,3-*d*]pyrimidine-6,8,10(9*H*,11*H*)trione (4g)

White solid, yield: 0.379 g (95%), mp >300°C. IR (KBr) (ν_{max}/cm^{-1}): 3019, 2952, 1701, 1673, 1623, 1571, 1509, 1446, 1356, 767. ^{1}H-NMR: δ = 2.24 (s, 3H, CH_3), 3.25 (s, 3H, NCH_3), 3.49 (s, 3H, NCH_3), 7.28 (br s, 4H, H—Ar), 7.60 (t, 1H, J = 7.4 Hz, H—Ar), 7.68 (d, 1H, J = 8.0 Hz, H—Ar), 7.90 (t, 1H, J = 7.0 Hz, H—Ar), 8.09 (d, 1H, J = 7.0 Hz, H—Ar) ppm. ^{13}C-NMR: δ = 21.4, 27.1, 29.4,

105.6, 113.2, 114.0, 117.8, 122.1, 124.6, 127.1, 129.3, 132.1, 133.3, 136.5, 137.2, 140.9, 142.8, 151.2, 156.0, 168.7, 172.9 ppm. Anal. Calcd for $C_{23}H_{17}N_3O_4$ (399.40): C, 69.17; H, 4.29; N, 10.52. Found: C, 69.35; H, 4.44; N, 10.38.

2.5.8 | 9,11-Dimethyl-7-(3-nitrophenyl)-6*H*-[1]benzopyrano[3′,4′:5,6]pyrido[2,3-*d*]pyrimidine-6,8,10(9*H*,11*H*)trione (4h)

Pale yellow solid, yield: 0.417 g (97%), mp >300°C. IR (KBr) (ν_{max}/cm^{-1}): 3008, 2984, 1704, 1676, 1610, 1572, 1520, 1485, 1346, 758. ^{1}H-NMR: δ = 3.27 (s, 3H, NCH_3), 3.53 (s, 3H, NCH_3), 7.69 (m, 1H, H—Ar), 7.75 (d, 1H, J = 7.6 Hz, H—Ar), 7.85 (t, 1H, J = 8.0 Hz, H—Ar), 7.97 (m, 2H, H—Ar), 8.15 (d, 1H, J = 7.7 Hz, H—Ar), 8.24 (br s, 1H, H—Ar), 8.35 (d, 1H, J = 8.1 Hz, H—Ar) ppm. ^{13}C-NMR: δ = 27.2, 29.3, 105.2, 112.1, 113.5, 114.6, 116.1, 117.7, 124.3, 125.6, 128.4, 129.5, 137.5, 138.6, 140.9, 141.2, 142.6, 151.1, 155.4, 156.8, 168.4, 174.1 ppm. Anal. Calcd for $C_{22}H_{14}N_4O_6$ (430.37): C, 61.40; H, 3.28; N, 13.02. Found: C, 61.48; H, 3.17; N, 12.88.

2.5.9 | 6-Amino-5-[(4-hydroxy-2-oxo-2*H*-[1]benzopyran-3-yl)(4-chlorophenyl)methyl]-1,3-dimethyl-2,4(1*H*,3*H*)-pyrimidinedione (5c)

White solid, yield: 0.418 g (95%), mp 190–192°C (lit: 193–194°C[41]). IR (KBr) (ν_{max}/cm^{-1}): 3445, 3361, 3240, 1696, 1663, 1618, 1570, 1509. ^{1}H-NMR: δ = 3.16 (s, 3H, CH_3), 3.40 (s, 3H, CH_3), 5.63 (s, 1H, H-7), 7.20 (d, J = 8.1 Hz, 2H, H—Ar), 7.29 (d, J = 8.1 Hz, 2H, H—Ar), 7.36 (br s, 2H, NH_2), 7.38 (t, J = 8.0 Hz, 1H, H—Ar), 7.45 (d, J = 8.0 Hz, 1H, H—Ar), 7.67 (t, J = 7.8 Hz, 1H, H—Ar), 7.86 (d, J = 7.8 Hz, 1H, H—Ar), 14.98 (s, 1H, OH) ppm. ^{13}C-NMR: δ = 29.1, 31.4, 36.6, 63.7, 87.4, 105.4, 117.0, 117.8, 124.6, 125.2, 126.1, 128.8, 129.4, 131.2, 133.4, 138.4, 150.9, 152.9, 156.1, 164.7, 165.0, 166.5 ppm. Anal. Calcd for $C_{22}H_{18}ClN_3O_5$ (439.85): C, 60.08; H, 4.13; N, 9.55. Found: C, 60.12; H, 4.19; N, 9.46.

3 | RESULTS AND DISCUSSIONS

We began our study by the synthesis of the catalyst based on the procedure mentioned in Experimental section. In this study, two carbon precursors were used to synthesis of porous bio-graphene (gelatin and Arabic gum). Gelatin was selected as a carbon source with nitrogen-containing groups, which can form N-doped graphene. Also, Arabic gum was added to gelatin solution to create a special network by interaction between these two carbon sources. It can produce a porous graphene structure with high surface area and high charge density that are attractive for catalytic application. This porous bio-graphene was used as a catalyst support to immobilize molybdenum oxide. For stabilizing molybdenum oxide on the surface of graphene, molybdenum oxide is dissolved in hydrogen peroxide to obtain oxodiperoxo molybdenum. This molybdenum precursor is highly active, which can oxidize the surface of graphene and quickly react with the functional groups of graphene to immobilize on the surface of support.[42,43]

The FT-IR spectra of the synthesized bio-graphene and MoO_3/graphene catalyst are reported in Figure 2. In both spectra, the characteristic absorption peaks of graphene at 1756, 1628, and 1248 cm^{-1} can be assigned to the stretching modes of C═O, C═C, and C—OH, respectively. The deformation mode of C—O was also observed at 1112 cm^{-1}. These peaks have higher intensities in MoO_3/graphene, which determine the higher number of oxygen-containing groups in the presence of oxidative condition (peroxo solution). A broad peak at 3442 cm^{-1} corresponds to the O—H stretching vibration in both graphene and MoO_3/graphene spectra. Regarding the small number of N-dopants, the vibration of C—N bond is too weak. The additional sharp peak in the IR spectra of MoO_3/graphene situated at 901 cm^{-1}, clearly confirmed the formation of the Mo═O groups on the surface of graphene.

The XRD patterns of the synthesized bio-graphene and MoO_3/graphene (after calcination at 300°C for 1 h) are shown in Figure 3. All reflection peaks at 2θ = 13.37, 27.17, 29.3, 32.03, 38.17, 45.54, 51.05, and 56.7° can be readily indexed to the (020), (110), (040), (021), (060), (002), and (081) planes of orthorhombic MoO_3 on the surface of graphene, respectively (JCPDS05-0508). Accordingly, the position of the main peak of graphene nanosheets is appeared as a strong diffraction peak at about 2θ = 22°.

SEM images of the synthesized bio-graphene and MoO_3/graphene catalyst have been depicted in Figure 4a, b. The SEM study of bio-graphene reveals the stacked porous nanosheets (Figure 4a). Figure 3b shows the nanobelts of molybdenum oxide on the surface of graphene in the MoO_3/graphene catalyst.

Figure 5 points out the Raman spectra of the synthesized bio-graphene. Two distinct peaks at 1318 and 1578 cm^{-1} are corresponded to D and G bands of graphene. The D and the G bands are assigned to the sp^3 and sp^2 hybrid carbon structures in the graphene, respectively.

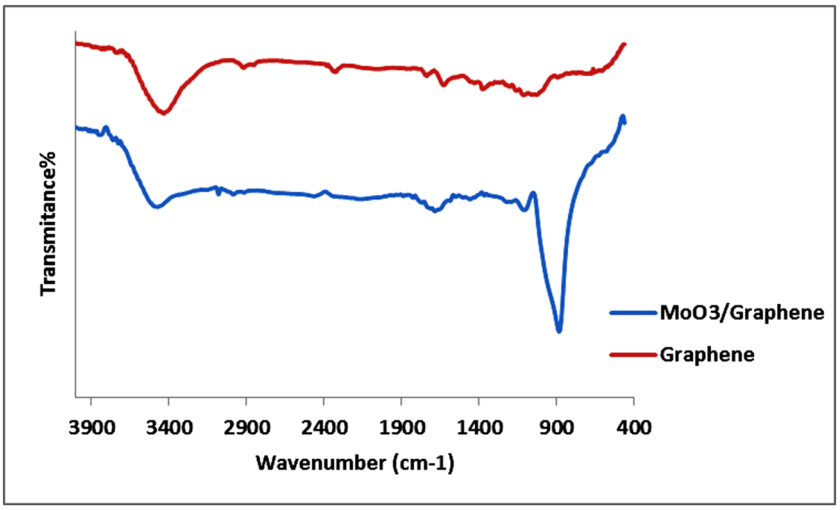

FIGURE 2 FT-IR spectra of the synthesized bio-graphene and graphene/MoO_3 nanocomposite

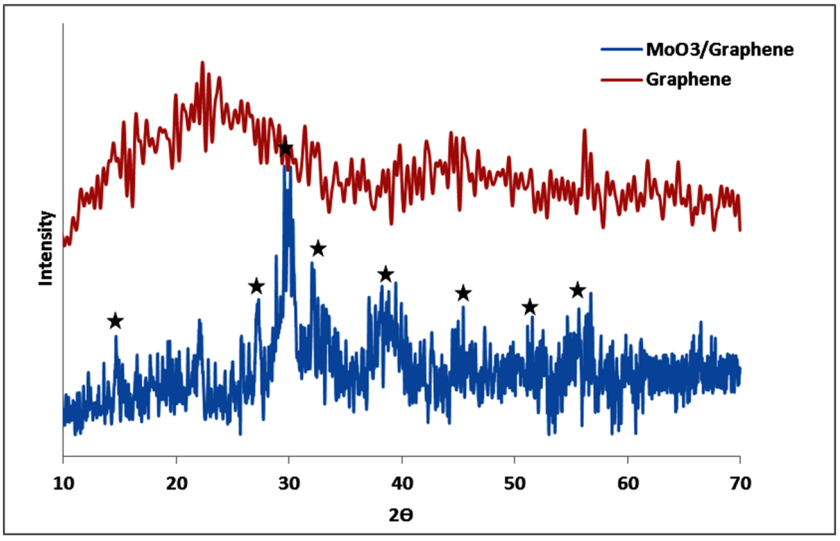

FIGURE 3 XRD patterns of the synthesized bio-graphene and graphene/MoO_3 nanocomposite

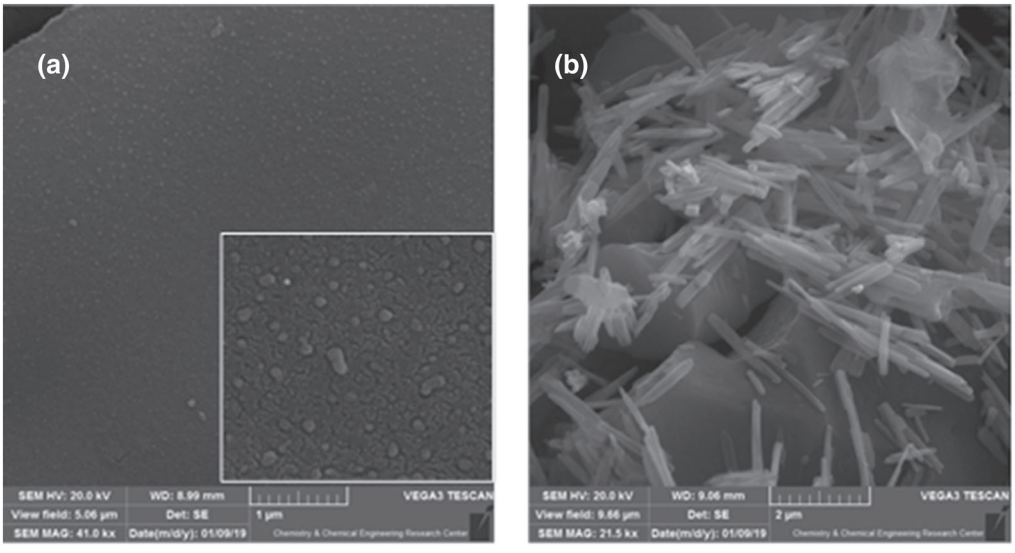

FIGURE 4 SEM images of (a) the synthesized bio-graphene and (b) graphene/MoO_3 nanocomposite

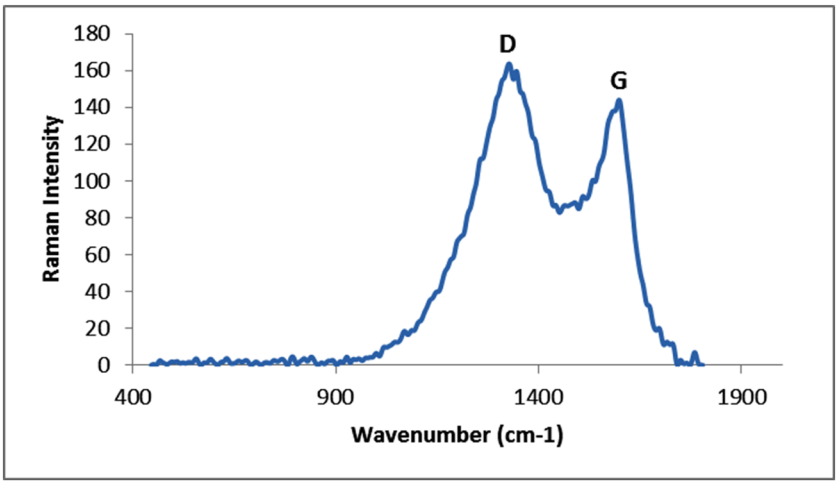

FIGURE 5 Raman spectra of the synthesized bio-graphene

To quantify the amount of molybdenum oxide on the MoO_3/graphene catalyst, thermogravimetric analysis (TGA/DTA) was done in the air (Figure 6). Result indicates that the synthesized bio-graphene is stable up to 400°C. The residue (10%) is corresponded to immobilized molybdenum oxide on the surface of graphene.

In the next runs, we sought to evaluate the various reaction conditions in the model reaction of 4-hydroxycoumarin (**1**), 4-chlorobenzaldehyde (**2c**), and 6-amino-1,3-dimethyluracil (**3**) for the synthesis of specific product **4c** (Scheme 2 and Table 1). The preliminary studies showed that in the absence of ultrasonic wave, the desired product **4c** was not observed, even under reflux conditions (Table 1, entries 1). This result occurs because the model reaction is stopped in the step of formation of uncyclized intermediate **5c**. The single crystal X-ray structure for **5c** (Figure 7) has previously been reported and illustrated the formation of intramolecular hydrogen bonds,[41] which prevents the further cyclization. Although by replacing two of the starting materials we could achieve these products,[40g,h] we also thought that an appropriate way to overcome this difficulty would be the use of ultrasonication. The conversion of the reactants into the desired product **4c** is mainly affected by using ultrasonic irradiation and the best results obtained in power of 70 W, in water at room temperature (Table 1, entries 2–4). Further investigation on the optimal quantity of the catalyst showed that only 0.05 g of the nanocomposite was efficient to give the best yield of product (97%) within 20 min under ultrasonic irradiation in water (Table 1, entries 3 and 5–7). Next, different catalysts were tested in the model reaction, but porous graphene/MoO_3 revealed to be must effective (Table 1, entries 3 and 8–9). To explore the effect of the reaction media, several solvents including EtOH, CH_2CL_2, CH_3CN, and DMF were examined. As expected, water was superior to push the reaction forward (Table 1, entries 3 and 9–13).

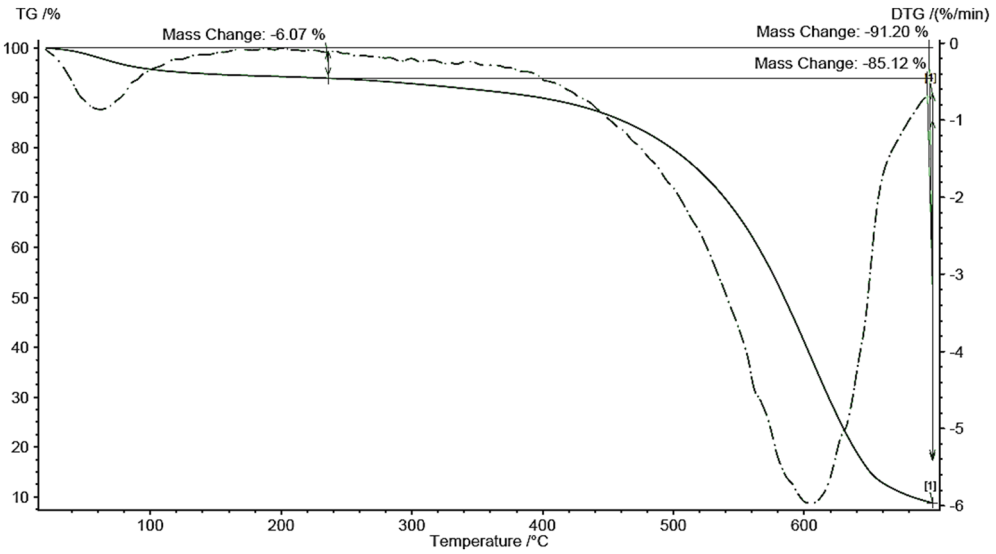

FIGURE 6 TGA/DTA analysis of the graphene/MoO_3 nanocomposite

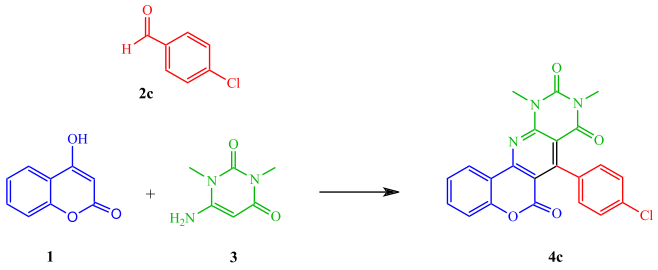

SCHEME 2 Synthesis of 7-(4-chlorophenyl)-9,11-dimethyl-6*H*-[1]benzopyrano[3′,4′:5,6]pyrido[2,3-*d*]pyrimidine-6,8,10(9*H*,11*H*)-trione (**4c**) as model reaction for the screening of the optimized reaction conditions

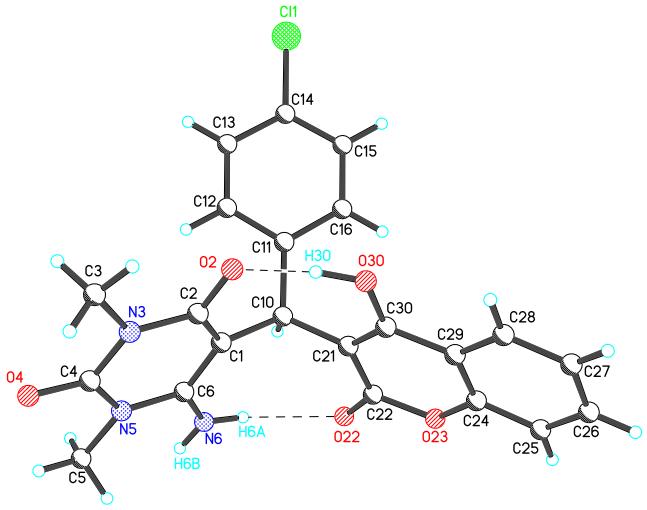

FIGURE 7 Single crystal X-ray structure of (**5c**) illustrating intramolecular hydrogen bond formation

To check the recyclability the catalyst was recovered by a simple procedure as described in the general procedure and successfully used in four consecutive cycles for the model reaction with a negligible loss of activity (Table 2).

On the basis optimization results obtained, the scope of this novel efficient method was explored by treating a range of various substituted benzaldehydes with 4-hydroxycoumarin and 6-amino-1,3-dimethyluracil to form the corresponding products in high yields (Table 3). Due to the volatile nature of most aliphatic aldehydes and therefore reduced product yields, we used only aromatic aldehydes in this reaction. It is noticeable that the substituent's effect on the aromatic ring did not show special effects in terms of yields under these reaction conditions. This may be due to the speed of the first step of the reaction in the formation of the alkene.

In accordance with the previous studies, a simplest and plausible mechanism for the present reaction is illustrated in Scheme 3. First, the mechanism proceeds by Knoevenagel condensation, as the MoO_3 possesses strong

TABLE 1 Optimization of reaction conditions for the synthesis of 7-(4-chlorophenyl)-9,11-dimethyl-6*H*-[1]benzopyrano[3′,4′:5,6]pyrido[2,3-*d*]pyrimidine-6,8,10(9*H*,11*H*)-trione (**4c**)

Entry	Catalyst (g)	Solvent (conditions)	US[a] power (W)	Time (min)	Yield (%)[b],[c]
1	Porous graphene/MoO_3 (0.05)	H_2O (Reflux)	—	240	—
2	Porous graphene/MoO_3 (0.05)	H_2O (US)	65	20	91
3	Porous graphene/MoO_3 (0.05)	H_2O (US)	70	20	97
4	Porous graphene/MoO_3 (0.05)	H_2O (US)	80	20	97
5	No catalyst	H_2O (US)	70	20	55
6	Porous graphene/MoO_3 (0.04)	H_2O (US)	70	20	74
7	Porous graphene/MoO_3 (0.06)	H_2O (US)	70	20	98
8	*p*-TsOH[a] (0.05)	H_2O (US)	70	20	85
9	DAHP[b] (0.05)	H_2O (US)	70	20	80
10	Porous graphene/MoO_3 (0.05)	EtOH (US)	70	20	92
11	Porous graphene/MoO_3 (0.05)	CH_2Cl_2 (US)	70	20	79
12	Porous graphene/MoO_3 (0.05)	CH_3CN (US)	70	20	83
13	Porous graphene/MoO_3 (0.05)	DMF[c] (US)	70	20	90

[a]*p*-TsOH, *p*-toluenesulfonic acid.
[b]DAHP, diammonium hydrogen phosphate.
[c]DMF, dimethylformamide.
[d]US, Ultasonic irradiation.
[e]Isolated yield.
[f]Reaction conditions: A mixture of 4-hydroxycoumarin (**1**, 1 mmol), 4-chlorobenzaldehyde (**2c**, 1 mmol), and 6-amino-1,3-dimethyluracil (**3**, 1 mmol) were kept at various reaction conditions.

TABLE 2 Recyclability of porous graphene/MoO_3 for the synthesis of 7-(4-chlorophenyl)-9,11-dimethyl-6*H*-[1]benzopyrano[3′,4′:5,6]pyrido[2,3-*d*]pyrimidine-6,8,10(9*H*,11*H*)-trione (**4c**) under optimized reaction conditions

Runs	Fresh	1	2	3	4
Isolated yield (%)[a], [b]	97	97	96	96	95

[a]Isolated yield.
[b]Reaction conditions: A mixture of 4-hydroxycoumarin (**1**, 1 mmol), 4-chlorobenzaldehyde (**2c**, 1 mmol), 6-amino-1,3-dimethyluracil (**3**, 1 mmol), and porous graphene/MoO_3 (0.05 g) in H_2O (3 ml) was sonicated at room temperature for 20 min at power of 70 W.

TABLE 3 Ultrasonic assisted porous graphene/MoO_3 catalyzed synthesis of 7-aryl-9,11-dimethyl-6*H*-[1]benzopyrano[3′,4′:5,6]pyrido[2,3-*d*]pyrimidine-6,8,10(9*H*,11*H*)-triones **4a**–**4h** in water

Products	Ar	Yield (%)[a],[b]	mp (°C)
4a	C_6H_5	95	>300
4b	4-Br-C_6H_4	98	>300
4c	4-Cl-C_6H_4	97	>300
4d	4-NC-C_6H_4	98	>300
4e	3-HO-C_6H_4	97	>300
4f	4-CH_3O-C_6H_4	98	>300
4g	4-CH_3-C_6H_4	95	>300
4h	3-O_2N-C_6H_4	97	>300

[a]Yields refer to those of pure isolated products characterized by IR, ^{1}H NMR, and ^{13}C NMR spectral data and by elemental analyses.
[b]Reaction conditions: A mixture of 4-hydroxycoumarin (**1**, 1 mmol), aromatic aldehyde (**2**, 1 mmol), 6-amino-1,3-dimethyluracil (**3**, 1 mmol), and porous graphene/MoO_3 (0.05 g) in H_2O (3 ml) was sonicated at room temperature for 20 min at power of 70 W.

acidic sites, which promote the reaction by coordinating to the oxygen of aromatic aldehydes **2** and activating it for nucleophilic attack to 6-amino-1,3-dimethyluracil **3** to generate alkene **6**. This in turn reacts with 4-hydroxycoumarin **1** via Michael addition to produce the uncyclized intermediate **5**. Intramolecular cyclization of **5** gives product **4**, after dehydration and aromatization. In order to demonstrate the proposed mechanism, we tried the model reaction into two separate steps (Scheme 3). In the first step and in the absence of 4-hydroxycoumarin **1**, the alkene **6c** formation is occurred from the reaction of 6-amino-1,3-dimethyluracil **3** with 4-chlorobenzaldehyde **2c**. When we used preformed alkene **6c** in the reaction with 4-hydroxycoumarin **1** in the second step, it shows that the product **4c** was given. As a result, the product formed in the first step is the intermediate obtained from the mentioned reaction performing in a one-pot three-component approach about 0.5 h after the start, confirmed by TLC.

4 | CONCLUSION

In summary, we have reported an operationally simple and green synthesis of 7-aryl-9,11-dimethyl-6*H*-[1]benzopyrano[3′,4′:5,6]pyrido[2,3-*d*]pyrimidine-6,8,10(9*H*,11*H*)-triones via cyclocondensation reaction of 4-hydroxycoumarin, aromatic aldehydes, and 6-amino-1,3-dimethyluracil catalyzed by porous graphene/MoO_3 nanocomposite. The porous graphene/MoO_3 nanocomposite was synthesized through a new facile route and characterized by FT-IR, XRD, SEM, Raman

SCHEME 3 The proposed mechanism for the formation of **4**

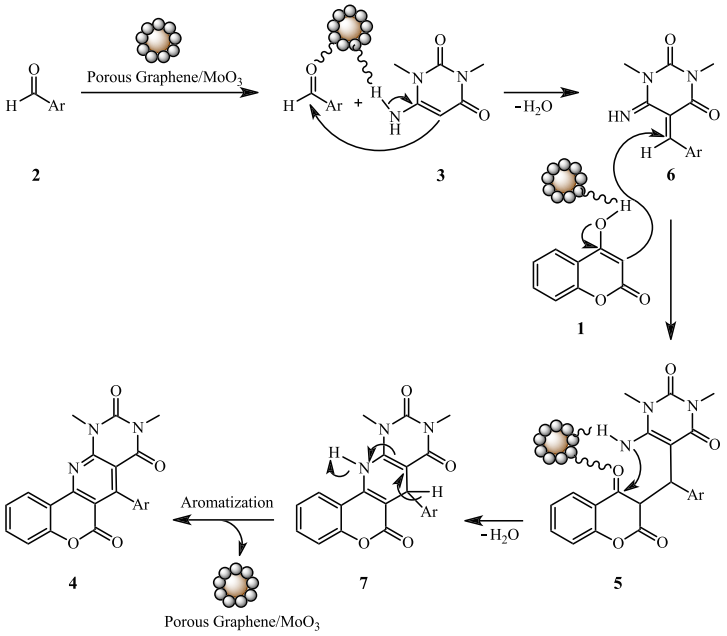

spectroscopy, and TGA analysis. The structures of target compounds **4a–4h** were also confirmed by IR, ^{1}H NMR, and ^{13}C NMR spectroscopic data and also by elemental analyses. High yields of products, short reaction times, the use of green solvent and reusable catalyst, and easy work-up are the main advantages of this protocol. Compared with heating method, ultrasound irradiation not only accelerates the reaction but is also necessary for the formation of the final cyclized product.

DATA AVAILABILITY STATEMENT

The data that support the findings of this study are available in the supporting information of this article.

ACKNOWLEDGEMENT

Shahrzad Abdolmohammadi is grateful to the Research Council of East Tehran Branch, Islamic Azad University, for financial support.

AUTHOR CONTRIBUTIONS

maryam afsharpour: Formal analysis.

ORCID

Shahrzad Abdolmohammadi https://orcid.org/0000-0001-8187-9624
Maryam Afsharpour https://orcid.org/0000-0002-5672-7546

REFERENCES

[1] Y. Q. Liu, L. H. Li, L. Yang, H. Y. Li, *Chem. Pap.* **2010**, *64*, 533.
[2] M. Mečiarovč, V. Poláčková, Š. Toma, *Chem. Pap.* **2002**, *56*, 208.
[3] M. Mečiarovč, Š. Toma, P. Babiak, *Chem. Pap.* **2004**, *58*, 104.
[4] K. Tabatabaeian, M. Mamaghani, N. O. Mahmoodi, A. Khorshidi, *Cat. Com.* **2008**, *9*, 416.
[5] B. A. Song, G. P. Zhang, S. Yang, D. Y. Hu, L. H. Jin, *Ultrason. Sonochem.* **2006**, *13*, 139.
[6] T. J. Mason, *Chem. Soc. Rev.* **1997**, *26*, 443.
[7] R. Mawson, M. Gamage, N. S. Terefe, K. Knoerzer, Ultrasound Technol. Food Bioprocess, **2011**, 369.
[8] S. Sharma, S. Gangal, A. Rauf, *Rasayan J. Chem.* **2008**, *1*, 693.
[9] N. Parikh, D. Kumar, S. R. Roy, A. K. Chakraborti, *Chem. Commun.* **2011**, *47*, 1797.
[10] G. Sharma, R. Kumar, A. K. Chakraborti, *Tetrahedron Lett.* **2008**, *49*, 4269.
[11] A. K. Chakraborti, S. Rudrawar, K. B. Jadhav, G. Kaur, S. V. Chankeshwara, *Green Chem.* **2007**, *9*, 1335.
[12] S. V. Chankeshwara, A. K. Chakraborti, *Org. Lett.* **2006**, *8*, 3259.
[13] G. L. Khatik, R. Kumar, A. K. Chakraborti, *Org. Lett.* **2006**, *8*, 2433.
[14] (a) C. Burda, X. Chen, R. Narayanan, M. A. El-Sayed, *Chem. Rev.* **2005**, *105*, 1025. (b) A. Y. Kim, H. J. Lee, J. C. Park, H. Kang, H. Yang, H. Song, K. H. Park, *Molecules* **2009**, *14*, 5169. (c) K. S. Lin, C. Y. Pan, S. Chowdhury, M. T. Tu, W. T. Hong, C. T. Yeh, *Molecules* **2011**, *16*, 348. (d) A. Monopoli, A. Nacci, V. Calò, F. Ciminale, P. Cotugno, A. Mangone, L. C. Giannossa, P. Azzone, N. Cioffi, *Molecules* **2010**, *15*, 4511. (e) F. K. Esfahani, D. Zareyee, R. Yousefi, *ChemCatChem* **2014**, *6*, 3333. (f) F. K. Esfahani, D. Zareyee, A. S. Rad, S. Taher-Bahrami, *Appl. Organomet. Chem.* **2017**, *31*, e3865.
[15] (a) M. Salavati-Niasari, *Micropor. Mesopor. Mat.* **2006**, *95*, 248. (b) M. Salavati-Niasari, A. Sobhani, F. Davar, *J. Alloys Compd.* **2010**, *507*, 77. (c) M. Yousefi, F. Gholamian, D. Ghanbari, M. Salavati-Niasari, *Polyhedron* **2011**, *30*, 1055. (d) M. Salavati-Niasari, D. Ghanbari, M. R. Loghman-Estarki, *Polyhedron* **2012**, *35*, 149. (e) M. Sabet, M. Salavati-Niasari, O. Amiri, *Electrochim. Acta* **2014**, *117*, 504. (f) S. Mortazavi-Derazkola, S. Zinatloo-Ajabshir, M. Salavati-Niasari, *Ceram. Int.* **2015**, *41*, 9593. (g) D. Ghanbari, M. Salavati-Niasari, *J. Ind. Eng. Chem.* **2015**, *24*, 284.
[16] N. M. Dimitrijevic, S. Tepavcevic, Y. Liu, T. Rajh, *J. Phys. Chem. C* **2013**, *117*, 15540.
[17] C. W. Peng, K. C. Chang, C. J. Weng, M. C. Lai, C. H. Hsu, S. C. Hsu, Y. Y. Hsu, W. I. Hung, Y. Wei, J. M. Yeh, *Electrochim. Acta* **2013**, *95*, 192.
[18] X. Wang, Y. Shen, A. Xie, L. Qiu, S. Li, Y. Wang, *J. Mater. Chem.* **2011**, *21*, 9641.
[19] L. Liang, J. Liu, C. F. Windisch Jr., G. J. Exarhos, Y. Lin, *Angew. Chem., Int. Ed.* **2002**, *41*, 3665.
[20] (a) S. Bose, T. Kuila, A. K. Mishra, R. Rajasekar, N. H. Kim, J. H. Lee, *J. Mater. Chem.* **2012**, *22*, 767. (b) Y. Huang, D. Chen, X. Hu, Y. Qian, D. Li, *Nanomaterials* **2018**, *8*, 431. (c) M. Afsharpour, Z. Dini, *Fuller. Nanotub. Car. N.* **2019**, *27*, 198. (d) M. Afsharpour, E. Khomand, *Int. J. Environ. Sci. Technol.* **2019**, *16*, 3125. (e) Z. Dini, M. Afsharpour, K. Tabarheidar, *Diamond Relat. Mater.* **2019**, *91*, 237. (f) G. Veréb, V. Kálmán, T. Gyulavári, S. Kertész, S. Beszédes, G. Kovács, K. Hernádi, Z. Pap, C. Hodúr, Z. László, *Water Supply* **2019**, *19*, 1167.
[21] (a) C. Huang, C. Li, G. Shi, *Energy Environ. Sci.* **2012**, *5*, 8848. (b) S. Gadipelli, Z. X. Guo, *Prog. Mater. Sci.* **2015**, *69*, 1. (c) M. Nasrollahzadeh, F. Babaei, P. Fakhri, B. Jaleh, *RSC Adv.* **2015**, *5*, 10782. (d) M. Nasrollahzadeh, M. Atarod, B. Jaleh, M. Gandomirouzbahani, *Ceram. Int.* **2016**, *42*, 8587. (e) S. Naghdi, B. Jaleh, N. Shahbaz, *Appl. Surf. Sci.* **2016**, *368*, 409. (f) P. Fakhri, H. Mahmood, B. Jaleh, A. Pegoretti, *Synth. Met.* **2016**, *220*, 653. (g) A. Omidvar, M. R. Rashidian Vaziri, B. Jaleh, N. Partovi Shabestari, M. Noroozi, *Chinese Phys. B* **2016**, *25*, 118102. (h) B. Jaleh, S. Habibi, M. Niyaifar, M. Nasrollahzadeh, *J. Mater. Sci.: Mater. Electron.* **2017**, *28*, 4974. (i) Y. Yildiz, T. Onal Okyay, B. Sen, B. Gezer, S. Kuzu, A. Savk, E. Demir, Z. Dasdelen, H. Sert, F. Sen, *ChemistrySelect* **2017**, *2*, 697. (j) S. Naghdi, M. Sajadi, M. Nasrollahzadeh, K. Y. Rhee, S. M. Sajadi, B. Jaleh, *J. Taiwan Inst. Chem. Eng.* **2018**, *86*, 158. (k) K. Yang, L. J. Huang, Y. X. Wang, Y. C. Du, J. G. Tang, Y. Wang, M. M. Cheng, Y. Zhang, M. J. Kipper, L. A. Belfiore, S. R. Wickramasinghe, *New J. Chem.* **2019**, *43*, 2846. (l) S. Majidi, B. Jaleh, B. Feizi Mohazzab, M. Eslamipanah, A. Moradi, *J. Inorg. Organomet. Polym. Mater.* **2020**, *30*, 3073.
[22] J. Zhu, H. Bienaymé, *Multicomponent Reactions*, Wiley-VCH, Weinheim **2005**.
[23] (a) B. M. Trost, *Acc. Chem. Res.* **2002**, *35*, 695. (b) P. A. Wender, V. A. Verma, T. J. Paxton, T. H. Pillow, *Acc. Chem.*

Res. **2008**, *41*, 40. (c) D. Zareyee, H. Alizadeh, *RSC Adv.* **2014**, *4*, 37941. (d) S. Farshbaf, L. Sreerama, T. Khodayari, E. Vessally, *Chem. Rev. Lett.* **2018**, *1*, 56. (e) F. Behmagham, Z. Asadi, Y. J. Sadeghi, *Chem. Rev. Lett.* **2018**, *1*, 68. (f) S. Zhi, X. Ma, W. Zhang, *Org. Biomol. Chem.* **2019**, *17*, 7632. (g) H. G. O. Alvim, J. R. Correa, J. A. F. Assumpção, W. A. da Silva, M. O. Rodrigues, J. L. de Macedo, M. Fioramonte, F. C. Gozzo, C. C. Gatto, B. A. D. Neto, *J. Org. Chem.* **2018**, *83*, 4044. (h) A. V. Vasco, Y. Méndez, A. Porzel, J. Balbach, L. A. Wessjohann, D. G. Rivera, *Bioconjugate Chem.* **2019**, *30*, 253. (i) L. S. da Silveira Pinto, M. R. C. Couri, M. V. N. de Souza, *Curr. Org. Synth.* **2018**, *15*, 21. (j) A. C. Boukis1, K. Reiter, M. Frölich, D. Hofheinz, M. A. R. Meier, *Nat. Commun.* **2018**, *9*, 1439. (k) M. Nikpassand, L. Zare Fekri, *Chem. Rev. Lett.* **2019**, *2*, 7. (l) F. Valinia, N. Shojaei, P. Ojaghloo, *Chem. Rev. Lett.* **2019**, *2*, 90. (m) E. Jafari, P. Farajzadeh, N. Akbari, A. Karbakhshzadeh, *Chem. Rev. Lett.* **2019**, *2*, 123.

[24] R. Pratap, V. J. Ram, *Chem. Rev.* **2014**, *114*, 10476.

[25] G. P. Ellis, in *The Chemistry of Heterocyclic Compounds Chromenes, Chromanes and Chromones*, (Eds: A. Weissberger, E. C. Taylor), John Wiley, New York **1977** 11 Chapter II.

[26] E. A. A. Hafez, M. H. Elnagdi, A. G. A. Elagamey, F. M. A. A. Ei-Taweel, *Heterocycles* **1987**, *26*, 903.

[27] M. M. Khafagy, A. H. F. A. El-Wahas, F. A. Eid, A. M. El-Agrody, *Farmaco* **2002**, *57*, 715.

[28] W. P. Smith, L. S. Sollis, D. P. Howes, C. P. Cherry, D. I. Starkey, N. K. Cobley, *J. Med. Chem.* **1998**, *41*, 787.

[29] A. Martinez-Grau, J. L. Marco, *J. Bioorg. Med. Chem. Lett.* **1997**, *7*, 3165.

[30] K. Hiramoto, A. Nasuhara, K. Michiloshi, T. Kato, K. Kikugawa, *Mutat. Res.* **1997**, *395*, 47.

[31] S. J. Mohr, M. A. Chirigos, F. S. Fuhrman, J. W. Pryor, *Cancer Res.* **1975**, *35*, 3750.

[32] C. P. Dell, C. W. Smith, European Patent Applications EP 537 949 21 Apr1. 993, Chemical Abstracts 119, 139102d, **1993**.

[33] G. Bianchi, A. Tava, *Agric. Biol. Chem.* **1987**, *51*, 2001.

[34] K. Mukai, K. Okabe, H. Hosose, *J. Org. Chem.* **1989**, *54*, 557.

[35] F. Eiden, F. Denk, *Arch. Pharm.* **1991**, *324*, 353.

[36] T. Ishikawa, *Heterocycles* **2000**, *53*, 453.

[37] C. D. Hufford, B. O. Oguntimein, D. Van Engen, D. Muthard, J. Clardy, *J. Am. Chem. Soc.* **1980**, *102*, 7365.

[38] V. Fuendjiep, A. E. Nkengfack, Z. T. Fomum, B. L. Sondengam, B. Bodo, *J. Nat. Prod.* **1998**, *61*, 380.

[39] J. Jean Wandji, Z. T. Fomum, F. Tillequin, F. Libot, M. Koch, *J. Nat. Prod.* **1995**, *58*, 105.

[40] (a) S. Abdolmohammadi, M. Mohammadnejad, F. Shafaei, *Z. Naturforsch. B* **2013**, *68*, 362. (b) S. Abdolmohammadi, *Curr. Catal.* **2013**, *2*, 116. (c) S. Abdolmohammadi, *Comb. Chem. High T. Scr.* **2013**, *16*, 32. (d) S. Abdolmohammadi, M. Afsharpour, S. Keshavarz-Fatideh, S. Afr, *J. Chem.-S. Afr. T.* **2014**, *67*, 203. (e) A. Rabiei, S. Abdolmohammadi, F. Shafaei, *Z. Naturforsch. B* **2017**, *72*, 241. (f) S. Khalilian, S. Abdolmohammadi, F. Nematolahi, *Lett. Org. Chem.* **2017**, *14*, 361. (g) A. Samani, S. Abdolmohammadi, A. Otaredi-Kashani, *Comb. Chem. High T. Scr.* **2018**, *21*, 111. (h) S. Abdolmohammadi, *Comb. Chem. High T. Scr.* **2018**, *21*, 594. (i) S. Fakheri-Vayeghan, S. Abdolmohammadi, R. Kia-Kojoori, *Z. Naturforsch. B* **2018**, *73*, 545. (j) S. Abdolmohammadi, Z. Hossaini, *Mol. Diversity* **2019**, *23*, 885. (k) S. Abdolmohammadi, B. Mirza, E. Vessally, *RSC Adv.* **2019**, *9*, 41868. (l) S. Abdolmohammadi, S. R. Rasouli Nasrabadi, M. R. Dabiri, S. M. Banihashemi Jozdani, *Appl. Organomet. Chem.* **2020**, *34*, e5462. (m) F. Chaghari-Farahani, S. Abdolmohammadi, R. Kia-Kojoori, *RSC Adv.* **2020**, *10*, 15614. (n) B. Saeedi, S. Abdolmohammadi, Z. MirJafari, R. Kia-Kojoori, *Monatsh. Chem.* **2020**, *151*, 773. (o) S. Abdolmohammadi, S. Shariati, N. Elmi Fard, A. Samani, *J. Heterocyclic Chem.* **2020**, *57*, 2729.

[41] S. Abdolmohammadi, S. Balalaie, M. Barari, F. Rominger, *Comb. Chem. High T. Scr.* **2013**, *16*, 150.

[42] M. Afsharpour, A. R. Amraee, *Mol. Catal.* **2017**, *436*, 285.

[43] M. Afsharpour, A. R. Mahjoub, M. M. Amini, *J. Nanosci. Nanotechnol.* **2010**, *10*, 6168.

SUPPORTING INFORMATION

Additional supporting information may be found online in the Supporting Information section at the end of this article.

How to cite this article: Abdolmohammadi S, Afsharpour M. An ultrasound assisted cyclocondensation reaction for the efficient synthesis of [1]benzopyranopyrido[*d*]pyrimidines using porous graphene/MoO_3. *Appl Organomet Chem*. 2020;e6028. https://doi.org/10.1002/aoc.6028